J Seismol (2010) 14:761–768
DOI 10.1007/s10950-010-9198-3

ORIGINAL ARTICLE

Magnitude scaling relationships from the first 3 s of P-wave arrivals in South Korea

Yongcheol Park · Sun-Cheon Park · Kwang-Hee Kim · Minkyu Park · Joohan Lee

Received: 27 July 2009 / Accepted: 6 June 2010 / Published online: 23 June 2010

Abstract Two empirical magnitude scaling relationships, predominant period ($\tau_p^{\max}$) and peak ground displacement (Pd) magnitudes, were investigated for the first 3 s after P-wave arrivals using 1,412 vertical waveforms recorded by the Korea National Seismic Network (KNSN) between 2001 and 2007. To evaluate the accuracy of the derived magnitude relationships, we simulated off-line ElarmS tests using 65 events occurring inside the KNSN. While the average magnitude error was ~0.70 magnitude units when using only the closest station to the epicentre, the error dropped to ~0.62 and ~0.42 magnitude units when using the closest two and closest four stations, respectively. For events $M_L \geq 3.0$, the average magnitude error was ~0.33 and showed stable values when the closest four stations were available. Our magnitude scaling relationships may be useful for initial work in developing an earthquake early warning system in South Korea.

Keywords P wave magnitude · Earthquake early warning · Earthquake location · Seismic array

Y. Park (✉) · M. Park · J. Lee
Division of Polar Earth-System Sciences,
Korea Polar Research Institute,
Incheon, South Korea
e-mail: ypark@kopri.re.kr

S.-C. Park
National Institute of Meteorological Research,
Seoul, South Korea

K.-H. Kim
Korea Ocean Research and Development Institute,
Ansan, South Korea

1 Introduction

The Korean Peninsula, the southeastern part of the Sino-Korean Craton, is located between the Japan and Ryukyu subduction zones and the northern China plate. Unlike neighbouring regions in China and Japan, where many large damaging earthquakes have occurred, the Korean Peninsula has very low earthquake activity (Giardini et al. 1999). The Korea Meteorological Administration (KMA) has reported that the Korean Peninsula experiences approximately 50 seismic events above $M_L = 2.0$/year, and most of which are less than $M_L = 4.0$. Studies of historical earthquakes, however, have shown that many significant, damaging earthquakes ($M \geq 7.0$) have occurred in the Seoul and Pusan regions (Chiu and Kim 2004; Lee et al. 2003; Lee and Yang 2006), where more than 20 million people currently live. The largest earthquake to occur in the Korean Peninsula during the twentieth century was reported by the State Seismological Bureau, Beijing, China (Engdahl and Villaseño 2002). The event occurred on 19 March 1952 at 38.5° N, 126.5° E,

with a reported magnitude (M_S) of 6.5. Unfortunately, because this earthquake occurred during the Korean War (1950–1953), no seismic records were obtained from the Korean Peninsula. Recently, two moderate earthquakes, the Odaesan event ($M_L = 4.8$, 20 January 2007) and the Uljin event ($M_L = 5.2$, 20 May 2004), have occurred (Fig. 1). The epicentre of the Uljin event was ~80 km away from a nuclear power plant. In addition, several events akin to 'earthquake swarms' were observed in the area during 2006.

The importance of mitigating potential damage to South Korea's infrastructure from seismic disturbances has become increasingly important, especially with the development of nuclear power facilities, high-speed railways, supercomputer centres, schools and high-technology centres. Modern seismometers and real-time telemetric technology are widely available and have been developed into earthquake early warning systems used to mitigate seismic hazards in urban and industrial areas of California (Allen 2006; Allen et al. 2009; Allen and Kanamori 2003; Wu et al. 2007; Wurman et al. 2007), Japan (Horiuchi et al. 2005; Kamigichi 2004), Romania (Wenzel et al. 1999), Taiwan (Wu and Kanamori 2005a; Wu and Teng 2002; Wu et al. 2006), Turkey (Alcik et al. 2009; Erdik et al. 2003), Mexico (Espinosa-Aranda et al. 1995) and Southern Italy (Olivieri et al. 2008; Zollo et al. 2009). To reduce the potential damage, a large earthquake may inflict upon a nuclear power facility or high-speed railway, the KMA intends to build an earthquake early warning system in South Korea. It is essential that any earthquake early warning system be able to rapidly determine the size and location of an earthquake.

2 Data

In South Korea, the switch from analogue to digital seismic monitoring started in 1998 after the Youngwol ($M_L = 4.5$) and Kyungju ($M_L = 4.2$) earthquakes of 1996 and 1997, respectively. Since then, the KMA has increased the number of seismic stations and upgraded instruments to create the Korea National Seismic Network (KNSN). Currently, the KNSN consists of 13 broadband,

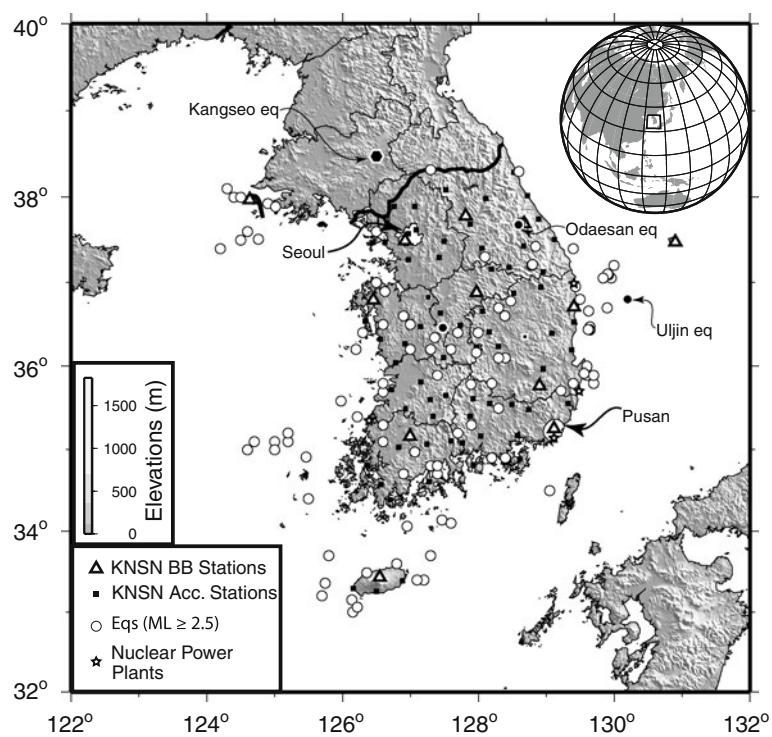

Fig. 1 Map of South Korea showing the locations of the earthquakes and seismic stations used in this study. *Thick* and *thin lines* represent the national boundary between North and South Korea and province boundaries, respectively. The metropolis areas of Seoul and Pusan are shown by *white polygons*. *Black circles* indicate the Odaesan and Uljin earthquakes, and a *hexagon* indicates the Kangseo event

31 short-period and 109 accelerometer stations equipped with Streckeisen STS-1 and STS-2, Kinemetrics SS-1 and Guralp CMG 40T-1, and Kinemetrics Episensor accelerographs. Continuous signals are digitized at 100 samples per second with 24-bit resolution at each station and transferred to the KMA earthquake monitoring division. Generally, waveforms stimulated from earthquake greater than $M = 6$ are clipped off when the epicentral locations are too close (~70 km) to seismic stations (Yun et al. 2005). The KNSN broadband stations are operated with accelerometers also to avoid the instrumental saturation on broadband sensors.

The KMA reports an annual earthquake catalogue based on the KNSN observations and using a local magnitude system. We used the digital waveform data of 300 earthquakes greater than $M_L = 2.5$ recorded by broadband and accelerometer stations between 2001 and 2007 (Fig. 1). A total of 1,412 vertical KNSN records were used to assess the relationships of earthquake magnitude to the frequency content (τ_p) and the maximum amplitude (Pd) within the first 3 s of the first P-wave arrival. In this study, we grouped the events into 0.3 magnitude intervals generally corresponding to the mean error on local magnitude. The 0.3 binning procedure averages out azimuthal effects such as radiation pattern, fault mechanism, etc. over events in the same magnitude occurring on different faults (Zollo et al. 2006).

3 Analysis and results

3.1 The relationship of magnitude and predominant period

Real-time observation of the predominant period ($\tau_p^{\max}$) has been described by Nakamura (1988) and has been used to determine earthquake magnitude in ElarmS, the earthquake early warning system used in California, USA (Allen and Kanamori 2003; Olson et al. 2005; Allen 2007; Wurman et al. 2007; Allen et al. 2009). To obtain the magnitude-period scaling relationship for South Korea, we used broadband and acceleration data. Acceleration data were integrated to velocity, and all data were low-pass filtered at 10 Hz using a recursive filtering method (Kanamori et al. 1999). Then, $\tau_p^{\max}$ was calculated from a waveform within 3 s of P-wave arrival using the recursive relation between the predominant period at time $i(\tau_i^P)$ and the ground motion recorded at time i (x_i): $\tau_i^P = 2\pi\sqrt{X_i/D_i}$, where X_i is the smoothed ground velocity squared ($X_i = \alpha X_{i-1} + x_i^2$), D_i is the smoothed velocity derivative squared ($D_i = \alpha D_{i-1} + (dx/dt)_i^2$), and α is a 1-s smoothing constant for 100 samples per second data ($\alpha = 0.95$) (Allen and Kanamori 2003; Allen 2007). The procedure of integrating waveforms magnified low frequency noises greater than their actual amplitude, and the $\tau_P^{\max}$ analysis is sensitive to signal to noise ratio (Fig. 2). Thus, estimated $\tau_P^{\max}$ values are scattered for the events with $M \leq 3.0$. Figure 3 shows a plot of individual waveform observations of $\tau_p^{\max}$ against M_L reported by the KMA along with the event averages. The $\tau_p^{\max}$ values from the single station per event are distributed widely (grey triangles in Fig. 3), but the average magnitudes of events $M_L \geq 3.0$ show a linear trend with M_L (stars in Fig. 3). Using the average $\tau_p^{\max}$ calculated from the velocity waveforms for the first 3 s after P-wave arrival, we determined the linear regression of magnitude against the dominant period $\tau_p^{\max}$ for South Korea:

$$\log\left(\tau_p^{\max}\right) = 0.156 M_L + 0.9797 \quad (1)$$

We determined the magnitude relation from Eq. 1:

$$M\left(\tau_p^{\max}\right) = 7.40 \log\left(\tau_p^{\max}\right) + 7.25 \quad (2)$$

The standard deviation of Eq. 1 is 0.11 s which is converted to ~0.16 magnitude units. For comparison, the best fit for small (M 3.8–5.0) and large earthquakes (M 5.0–7.4) in Japan is shown by the dotted and dashed lines, respectively. Our best-fit regression line is similar to the relationship for smaller events in Japan (Lockman and Allen 2007).

3.2 The relationship of magnitude and peak ground displacement

We used the relationship of P-wave peak ground displacement (Pd) within the first 3 s of P-wave

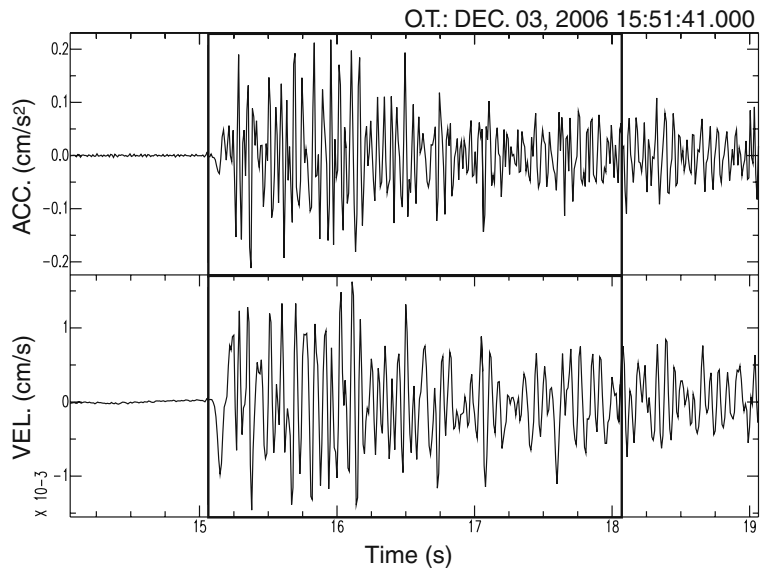

Fig. 2 Example of strong-motion records. The event magnitude is $M_L = 2.5$, and the epicentral distance is 81 km. *Upper trace* is raw data (acceleration trace) and *bottom* one shows integrated velocity motion. The time window indicates 3 s from the first P-wave arrival

arrival to provide an additional estimate of earthquake magnitude. Wu and Kanamori (2005b) suggested that P-wave peak ground velocity (*Pv*) and displacement (*Pd*) contain more long-period energy than P-wave peak ground acceleration (*Pa*) and that *Pd* in particular shows good correlation with peak amplitude parameters. The '*Pd* magnitude' method is used in earthquake warning systems in California, Taiwan, and Japan to reduce the overall magnitude error (e.g., Kamigichi 2004; Wu and Kanamori 2005b; Tsang et al. 2007; Wurman et al. 2007). Kamigichi (2004) introduced the following magnitude formula,

$$\log(Pd) = A + B \times M + C \times \log R + D \times R \quad (3)$$

where R is the distance between the station and the epicentre in kilometres. In Eq. 3, $C \times \log R$ and $D \times R$ represent amplitude decay corrections for geometric spreading and the Q effect, respectively. The Q effect is not significant within 200 km of an event, and $D \times R$ can be omitted to reduce unknowns (Allen 2007). The *Pd* amplitude also depends on the P-wave radiation pattern, and a good azimuthal coverage of Pd observations in the regression analysis is important. Based on Eq. 3, we determined a best-fit regression line with a $\log(Pd) - \log(R)$ relationship (Fig. 4).

$$\log(Pd) = 0.826 M_L - 1.256 \log(R) - 2.941 \pm 0.31 \quad (4)$$

From Eq. 4, we can estimate the magnitude from the *Pd*:

$$M(Pd) = 1.21 \cdot \log(Pd) + 1.52 \cdot \log(R) + 3.56 \quad (5)$$

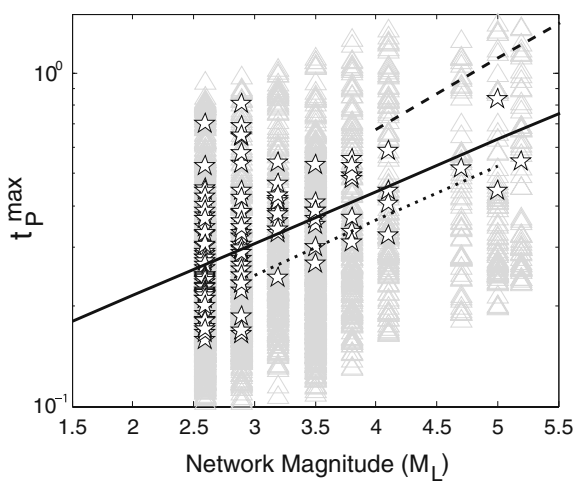

Fig. 3 The scaling relation between τ_p^{max} and M_L magnitude for earthquakes in South Korea. *Grey triangles* represent estimates for individual stations using the first 3 s of P-wave arrival. Average values are shown by *white stars*. The *solid line* shows the best-fit linear scaling relationship. *Dotted* and *dashed lines* indicate the respective scaling relationships derived from small and large earthquakes occurring in Japan, respectively (Lockman and Allen 2007)

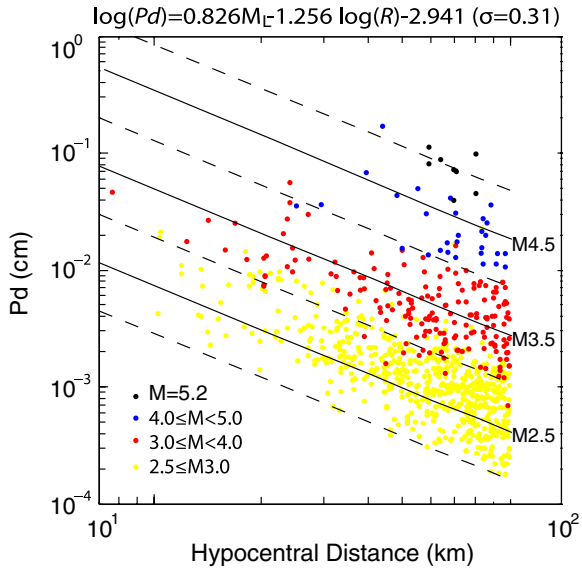

Fig. 4 Plot of Pd measurements. The *diagonal lines* show the computed linear log(Pd)-log(R) relationship, *solid lines* represent magnitude 2.5, 3.5 and 4.5, and *dashed lines* indicate magnitude 2, 3, 4 and 5

where *Pd* is in centimetres. Figure 5 shows a plot of the relationship between the magnitudes estimated from individual peak displacement observations from Eq. 5 and the local magnitudes reported by the KMA.

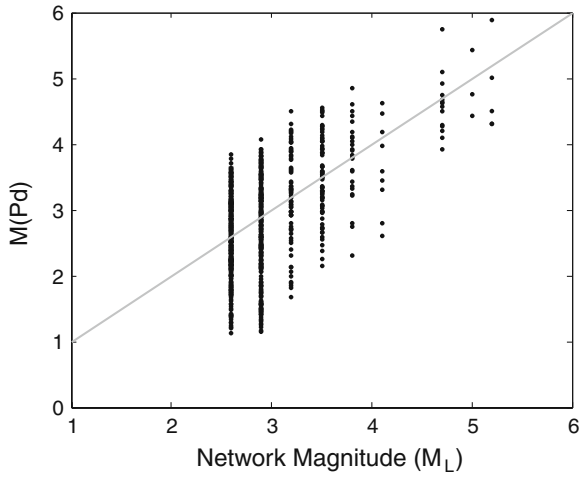

Fig. 5 The scaling relationship between Pd and ML magnitude for earthquakes in South Korea. Each point represents a magnitude estimated from an individual station measurement using the first 3 s of P-wave arrival. The *solid line* represents a 1:1 relationship between the estimated magnitude, M(Pd) and observed magnitude, ML

4 Application to ElarmS off-line tests

The primary objective of this study was to establish magnitude relationships for a real-time early warning system. For this purpose, and for evaluating the accuracy of the derived magnitude scaling relationships, we adapted the ElarmS methodology originally designed for an earthquake warning system in southern and northern California (Allen and Kanamori 2003; Allen 2007; Tsang et al. 2007; Wurman et al. 2007). Since the hypocentral depths of earthquakes occurring inside South Korea are small and range between ~2–15 km (KIGAM 2009), we fixed the hypocentral depths at 9 km and used a 1-D velocity model (Chang and Baag 2006) to determine event locations. The ElarmS system provides the first earthquake location from the first station and yields an initial magnitude estimate 1 s later. Subsequently, earthquake location and average magnitude are re-computed from all available stations every second. Allen (2007) and Wurman et al. (2007) have provided detail descriptions of the ElarmS methodology. The average magnitudes of the $\tau_p^{\max}$ and *Pd* scaling relationships were simulated through ElarmS off-line tests using 65 events.

Figure 6a shows the variation in magnitude error versus time for each event. Although magnitude errors fluctuate, most earthquakes showed stable magnitude errors after 11 s from their origin time (0 s in Fig. 6a). For events of $M_L < 3.0$, the maximum and average magnitude errors between ElarmS simulations and reported magnitude by KMA were 0.85 and 0.29 magnitude units, respectively (grey lines in Fig. 6). The maximum and average errors for events $M_L \geq 3.0$ were slightly smaller at 0.5 and 0.24 magnitude units, respectively (black lines in Fig. 6). We also evaluated the accuracy of the magnitude relationships according to the number of available stations. Figure 6b shows that error decreased as multiple stations were combined to calculate the average magnitude. The average magnitude error was ~0.70 magnitude units when only the closest station to the epicentre was used. The error dropped to ~0.62 and ~0.42 magnitude units using data from the closest two and four stations, respectively. For events of $M_L \geq 3.0$, the average magnitude error for was ~0.33 and

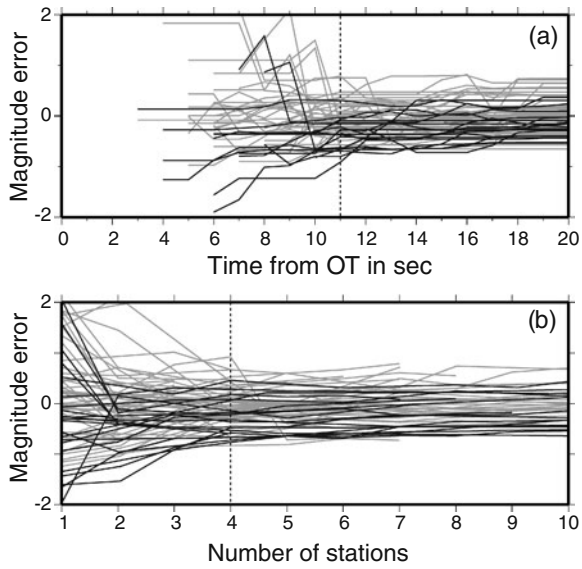

Fig. 6 Plots of magnitude errors vs. **a** time (s) from the event origin time and **b** the number of stations used to average magnitude for the first 3 s of P-wave arrival. *Grey* and *black lines* represent events below and above $M_{\mathrm{L}} = 3.0$, respectively. *Dotted lines* indicate the time at 11 s from the event origin time (**a**) and the magnitude error when using data from four stations (**b**)

showed stable value when the closest four stations were used.

5 Discussion and conclusions

The magnitude scaling relationships for $\tau_p^{\max}$ and *Pd* have been developed using the first 3 s of vertical broadband data after the initial P wave, collected by the KNSN between 2001 and 2007. Magnitude estimates using the data from one station had considerable error. Such error could be significantly reduced by taking the average of measurements from several stations. Figure 7 shows a plot of the associated magnitude measured with the four closest stations to an earthquake epicentre versus the network magnitude (M_{L}). The maximum magnitude errors were 0.5 and 0.8 magnitude units for events bigger and smaller than $M_{\mathrm{L}} = 3.0$, respectively.

The uncertainty of the event location is a critical factor in determining a *Pd* magnitude. KNSN stations are distributed throughout South Korea with ~35 km between any two adjacent stations that indicate the maximum initial epicentral distance error can be ~18 km in ElarmS test. Lancieri and Zollo (2008) analysed the importance of earthquake locations for estimating Pd magnitude using a probabilistic Bayesian approach, and showed their probabilistic algorithm is able to provide a robust estimation of the final magnitude and can deal with the magnitude saturation effect for events greater than $M = 7$. In ElarmS off-line simulation, our estimated magnitudes taking average values from the $\tau_p^{\max}$ and *Pd* magnitude relationships have stable magnitudes when four or more stations are used to determine magnitudes.

Considering the interval of KNSN stations and events occurring in KNSN, the ElarmS off-line simulations imply that when using the four closest stations, P-wave arrival can be detected within ~6 s for events occurring inside South Korea. In this study, we have shown that only 3 s of waveform data are required to estimate earthquake magnitude and that the potential telemetry delay time of the KNSN equipped with Q730, Q4120 and Q330 instruments is ~3 s. Therefore, we can estimate a reliable magnitude within 12 s. The KNSN system was not designed for early warning purposes, and there are considerable delays in data processing. However, the KMA keeps adding new stations to the KNSN, including borehole broadband stations, and intends to upgrade the KNSN to serve as an earthquake early warning system in the near future.

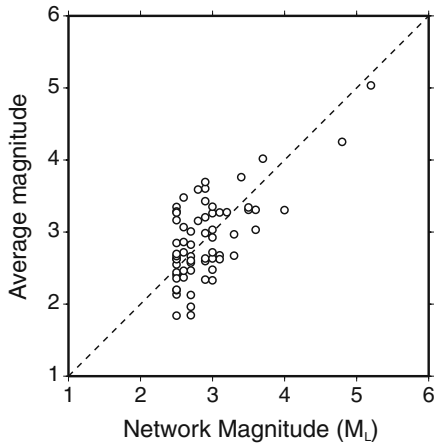

Fig. 7 Plot of average magnitude estimated with the four closest stations vs. network magnitude (ML). The *dashed line* on the plot represents a 1:1 relationship between the estimated magnitude and the observed magnitude

A critical question to ask of this earthquake early warning system is: can the magnitude relationships derived from smaller earthquakes (M_L 2.5–5.2) in South Korea be extrapolated to larger events? Previous studies optimized the sensitivity of the relationship between magnitude and τ_p^{max} using two different sets of low-pass-filtered data at 10 Hz for $M < 5.0$ and 3 Hz for $M > 4.5$ for events in southern California (Allen and Kanamori 2003) and at 5 Hz for $M < 5.0$ and 1 Hz for $M \geq 5.0$ for events in Japan (Lockman and Allen 2007). We attempted to derive the period-magnitude relationship from the 3 Hz low-pass-filtered data but could not find an appropriate relationship for Korean events (M_L 2.5–5.2). In the *Pd*-magnitude relationship for the network magnitude (M_L), *Pd* values are generally saturated for large events ($M > \sim 6.5$) (Wu et al. 2006; Zollo et al. 2006; Rydelek and Kim 2010) because the 3-s window from the first P arrivals is not sufficient for large earthquakes rupturing continuously over that time window. In addition, Rydelek and Kim (2010) compared *Va* (defined as the level at which the absolute value of $V \geq Va$ for a time duration of at least 0.3 s (Yamamoto et al. 2008) and peak ground displacement relationships estimated from small ($M_L \leq \sim 5.0$) and large earthquakes in Japan ($3.5 \leq M_{JMA} \leq 7.5$). They showed that the slope of the best-fit lines determined from small events was similar to that determined for large events in magnitude scaling factors but that the values of *Va* were ~5 times smaller for small events than for large ones. The dissimilarities in the magnitude scaling relationships between small and large events suggest that extrapolating a magnitude relationship for small events to large events can result in an underestimation of earthquake size and may result in missed alarms. As a result, our future research will attempt to calibrate factors that will enable us to apply our τ_p^{max} and *Pd* magnitude relationships to large magnitude earthquakes and improve the early warning system for large events in South Korea.

Acknowledgements We thank Dr. Yih-Min Wu, Dr. Aldo Zollo, and an anonymous reviewer for constructive comments. This work was funded by Korea Polar Research Institute (KOPRI) Grant PP10020. S. Park's contribution was performed under the auspices of the Korea Meteorological Administration under contract METRI-2010-B-5 (Study on Development and Application of Earthquake Monitoring Techniques).

References

Alcik H, Ozel O, Apaydin N et al (2009) A study on warning algorithms for Istanbul earthquake early warning system. Geophys Res Lett 36:L00B05. doi:10.1029/2008GL036659

Allen RM (2006) Probabilistic warning times for earthquake ground shaking in the San Francisco Bay area. Seismol Res Lett 77:371–376

Allen RM (2007) The ElarmS earthquake early warning methodology and application across California. In: Gasparini P, Manfredi G, Zschau J (eds) Earthquake early warning systems. Springer-Verlag, Berlin, Federal Republic of Germany, University of Napoli, Department of Physics, Naples, Italy, pp 21–43

Allen RM, Kanamori H (2003) The potential for earthquake early warning in Southern California. Science 300:786–789. doi:10.1126/science.1080912

Allen RM, Brown H, Hellweg M et al (2009) Real-time earthquake detection and hazard assessment by ElarmS across California. Geophys Res Lett 36:L00B08. doi:10.1029/2008GL036766

Chang S-J, Baag C-E (2006) Crustal structure in southern Korea from joint analysis of regional broadband waveforms and travel times. Bull Seismol Soc Am 96:856–870

Chiu J-M, Kim SG (2004) Estimation of regional seismic hazard in the Korean Peninsula using historical earthquake data between A.D. 2 and 1995. Bull Seismol Soc Am 94:269–284

Engdahl ER, Villaseño A (2002) The centennial catalog- global seismicity: 1900–1999. In: Lee HK, Jennings PC, Kisslinger C (eds) International handbook of earthquake and engineering seismology. Academic Press, pp 665–690. http://earthquake.usgs.gov/research/data/centennial.php

Erdik M, Fahjan Y, Ozel O et al (2003) Istanbul earthquake rapid response and the early warning system. Bulletin of Earthquake Engineering 1:157–163

Espinosa-Aranda JM, Jimenez A, Ibarrola G et al (1995) Mexico City seismic alert systerm. Seismol Res Lett 66:42–52

Giardini D, Grunthal G, Shedlock K et al (1999) Global Seismic Hazard Map (GSHAP). International decade on natural disaster reduction United Nations: http://www.seismo.ethz.ch/GSHAP

Horiuchi S, Negishi H, Abe K et al (2005) An automatic processing system for broadcasting earthquake alarms. Bull Seismol Soc Am 95:708–718

Kamigichi O (2004) JMA earthquake early warning. J Jpn Assoc Earthquake Eng 4:1–4

Kanamori H, Maechling P, Hauksson E (1999) Continuous monitoring of ground-motion parameters. Bull Seismol Soc Am 89:311–316

KIGAM (2009) KIGAM Korea earthquake online catalogue. http://quake.kigam.re.kr/pds/db/db.html

Lancieri M, Zollo A (2008) A Bayesian approach to the real-time estimation of magnitude from the early P and S wave displacement peaks. J Geophys Res 113: B12302. doi:10.1029/2007JB005386

Lee K, Yang W-S (2006) Historical seismicity of Korea. Bull Seismol Soc Am 96:846–855

Lee K, Chung NS, Chung TW (2003) Earthquakes in Korea from 1905 to 1945. Bull Seismol Soc Am 93:2131–2145

Lockman AB, Allen RM (2007) Magnitude-period scaling relations for Japan and the Pacific Northwest: implications for earthquake early warning. Bull Seismol Soc Am 97:140–150. doi:10.1785/0120040091

Nakamura Y (1988) On the urgent earthquake detection and alarm system (UrEDAS). In: Proceedings of ninth world conference on earthquake engineering, vol VII, pp 673–678

Olivieri M, Allen RM, Wurman G (2008) The potential for earthquake early warning in Italy using ElarmS. Bull Seismol Soc Am 98:495–503

Olson EL, Allen RM (2005) The deterministic nature of earthquake rupture. Nature 438:212–215. doi:10.1038/nature04214

Rydelek P, Kim K-H (2010) A study on feasibility of earthquake early warning in Korea: determination of locations and magnitudes of events. Geosci J 14:41–47

Tsang LLH, Allen RM, Wurman G (2007) Magnitude scaling relations from P-waves in southern California. Geophy. Res. Let. 34:L19304. doi:10.1029/2007GL031077

Wenzel F, Oncescu MC, Baur M et al (1999) An early warning system for Bucharest. Seismol Res Lett 70:161–169

Wu Y-M, Teng TL (2002) A virtual subnetwork approach to earthquake early warning. Bull Seismol Soc Am 92:2008–2018

Wu Y-M, Kanamori H (2005a) Experiment on an onsite early warning method for the Taiwan early warning system. Bull Seismol Soc Am 95:347–353. doi:10.1785/0120040097

Wu Y-M, Kanamori H (2005b) Rapid assessment of damage potential of earthquakes in Taiwan from the beginning of P Waves. Bull Seismol Soc Am 95:1181–1185. doi:10.1785/0120040193

Wu Y-M, Yen H-Y, Zhao L et al (2006) Magnitude determination using initial P waves: a single-station approach. Geophys Res Lett 33:L05306. doi:10.1029/2005GL025395

Wu Y-M, Kanamori H, Allen RM et al (2007) Determination of earthquake early warning parameters, τc and Pd, for southern California. Geophys J Int 170:711–717. doi:10.1111/j.1365–246X.2007.03430.x

Wurman G, Allen RM, Lombard P (2007) Toward earthquake early warning in Northern California. J Geophys Res 112:B08311

Yamamoto S, Rydelek P, Horiuchi S et al (2008) On the estimation of seismic intensity in earthquake early warning systems. Geophys Res Lett 35:L07302

Yun KH, Park DH, Choi WH et al (2005) Development of site-specific ground-motion attenuation relations for nuclear power plant sites and study on their characteristics. 2005 fall earthquake engineering society of Korea workshop earthquake engineering society of Korea

Zollo A, Lancieri M, Nielsen S (2006) Earthquake magnitude estimation from peak amplitudes of very early seismic signals on strong motion records. Geophys Res Lett 33:L23312. doi:10.1029/2006GL027795

Zollo A, Iannaccone G, Lancieri M et al (2009) Earthquake early warning system in southern Italy: methodologies and performance evaluation. Geophys Res Lett 36:L00B07. doi:10.1029/2008GL036689